



## Development of a Nanofiber Wound Dressing Prototype and Evaluation of in Vitro Biocompatibility

---

Emre Fatih Ediz, Cansu Güneş Çimen, Deniz Ümmetoğlu,  
Meltem Demirel Kars and Ahmet Avcı

EasyChair preprints are intended for rapid dissemination of research results and are integrated with the rest of EasyChair.

April 6, 2022

## Development of a Nanofiber Wound Dressing Prototype and Evaluation of In Vitro Biocompatibility

Emre Fatih EDİZ<sup>1,2\*</sup>, Cansu GÜNEŞ ÇİMEN<sup>3</sup>, Deniz ÜMMETOĞLU<sup>2</sup>, Meltem DEMİREL KARS<sup>3</sup>,  
Ahmet AVCI<sup>3</sup>

<sup>1</sup>Department of Nanoscience and Nanoengineering, Institute of Science, Necmettin Erbakan University, Turkey

<sup>2</sup>Zade & Zade Vital Ibn-i Sina R&D Center, Zade Vital Pharmaceuticals Inc., Turkey

<sup>3</sup>Department of Biomedical Engineering, Faculty of Engineering, Necmettin Erbakan University, Turkey

\*[emrefatihediz@gmail.com](mailto:emrefatihediz@gmail.com) ORCID ID 0000-0003-0259-4298

**Abstract** – In this study, it was aimed to develop a two-layer wound dressing prototype containing Polycaprolactone (PCL)/Collagen (COL) and PCL/St. John's Wort oil/*Momordica charantia* maceration oil, which will accelerate wound healing, minimize infection and provide a suitable moist environment. The evaluation of in-vitro biocompatibility of dressing was also aimed.

Scanning electron microscope (SEM) analyzes showed that PCL/COL containing fibers had a diameter of about 135 nm, while the diameter of nanofibers containing PCL/St. John's Wort oil/*Momordica charantia* maceration oil was approximately 513 nm. According to thermal and gravimetric analysis (TGA) results, thermal degradation temperature ranges of PCL/St. John's Wort oil/*Momordica charantia* maceration oil, PCL/COL and double layer nanofibers were found 275-410 °C, 300-430 °C and 350-440 °C, respectively. Weight losses due to temperature increase were found to be approximately 88.4%, 84.32% and 88.1% for PCL/St. John's Wort oil/*Momordica charantia* maceration oil, PCL/COL and double layer nanofibers, respectively. As an in vitro study, L929 normal fibroblast cells were grown with the wound dressing prototype for 24 hours, 72 hours, and 144 hours. Normal fibroblast cell proliferation was found to be 60.4%, 80.18% and 66.71% after 24, 72, and 144 hours incubation period, respectively.

**Keywords** – Electrospinning, Electrospun Nanofiber, *Hypericum perforatum*, *Momordica charantia*, Wound Dress

### I. INTRODUCTION

Skin wound healing is an extraordinary mechanism of cellular function involving the interaction of various cells, growth factors and cytokines. Physiological wound healing restores tissue integrity, but in most cases the process is limited to wound repair. Various ongoing studies in the literature aim to obtain more effective wound treatments in order to reduce costs, provide long-term relief and provide effective wound healing [1]. Wound bedspreads play an important role in wound healing management. They protect the wound from external factors and accelerate the healing process. On the basis of the wound healing mechanism, an ideal dressing should have some important characteristics. An ideal dressing should

absorb excess exudate, protect the wound from microbial infection, maintain a moist healing environment at the wound site, facilitate gas exchange and should be non-toxic, biocompatible and degradable, not adhere to the wound, and be easy to replace and remove [2-3]. Electrospun nanofibers for wound dressing are gaining intense interest due to their unique advantages. Nanofibers have high porosity with excellent pore connectivity, which is especially important for expelling fluid from the wound and allowing the breathing freely. The natural small pores and high specific surface area enable them to inhibit the invasion of exogenous microorganisms and help to control fluid drainage. The three-dimensional mesh scaffold structure of the fibers is similar to the

natural extracellular matrix, which can provide a similar cell growth microenvironment and is more conducive to wound healing [4].

*Momordica charantia* has antilipidemic, antibacterial, antiviral, and anticancer properties. Research is being conducted on the wound healing properties of *Momordica charantia* maceration oil. It has been observed that the amount of wound epithelialization increased due to the antimicrobial properties of the flavonoids it contains. St John's Wort, which is used in the treatment of internal and external diseases, contains hyperforin and biflavonoids, which have sedative, anti-ulcer, analgesic and anti-inflammatory properties, and are generally used in wound and burn treatments. St. John's Wort (*Hypericum perforatum*) has an important place in wound healing from ancient times to the present day. It contains trace amounts of amino acids, xanthone, tannins and essential oils, as well as biflavones, phenylpropanes, flavonoids, phloroglucinols, naphthodiantron and proanthocyanidins. Studies have reported that St. John's Wort has anti-inflammatory effects, increases infection resistance and fibroblast migration, and provides collagen deposition [5].

## II. MATERIALS AND METHOD

### A. Materials

Polycaprolactone (PCL,  $M_w=80.000$  g/mol), Dichloromethane (%99,5), Formic acid (% 85), Acetone (%99,5), DMEM (Medium with high glucose, L-Glutamine, phenol red, without HEPES), Fetal Bovine Serum, (qualified, heat inactivated, gentamycin solution, cell proliferation kit (XTT based) Cell Culture Plate, (96 well,)), Cell Culture Flask (25 cm<sup>2</sup>), Marine Collagen Type I, *Momordica Charantia* maceration oil, St. John's Wort Oil, Ethanol (%99) were used for experimental setup of study.

### B. Equipment

Electrospinning equipment consisting of a high voltage source, an aluminum rotary cylinder collector and four syringe pumps, Fourier Transform Infrared Spectroscopy (FTIR)(Shimadzu IRTracer-100, Japan), Field emission scanning electron microscope FE-SEM, ZEISS GeminiSEM 500, Germany), Thermogravimetric Analysis (Shimadzu Japan TGA-50), Tensile tester (Shimadzu AGS-X), CO<sub>2</sub> incubator, Class II sterile cabinet, centrifuge, 96-

well plate reader (Elisa reader Thermo-Skyhigh) were used.

### C. Method

To obtain nanofibers by electrospinning, firstly PCL and oils were dissolved in dichloromethane (100% (w/v) PCL, 2.5% St. John's Wort oil, 2.5% *Momordica charantia* maceration oil). For the second layer, 15% PCL and 15% collagen type I were prepared by dissolving in a mixture of formic acid: acetone (70:30). An electrospinning setup consisting of a high voltage source, an aluminum rotary cylinder collector and four syringe pumps was used to produce nanofibers.

The surface and physico-chemical properties of the produced nanofibers were characterized by FESEM, FTIR, TGA and mechanical tension test. The biocompatibility of the developed nanofiber dressing prototype was analyzed by XTT cytotoxicity test after culturing L929 fibroblast cells with nanofibers for 24, 72 and 144 hours.

## III. RESULTS

### A. Fourier Transform Infrared Spectroscopy (FTIR)

Produced PCL/COL, PCL/Yellow St. John's Wort Oil/ *Momordica charantia* Maceration Oil nanofibers were compared by FT-IR analysis.

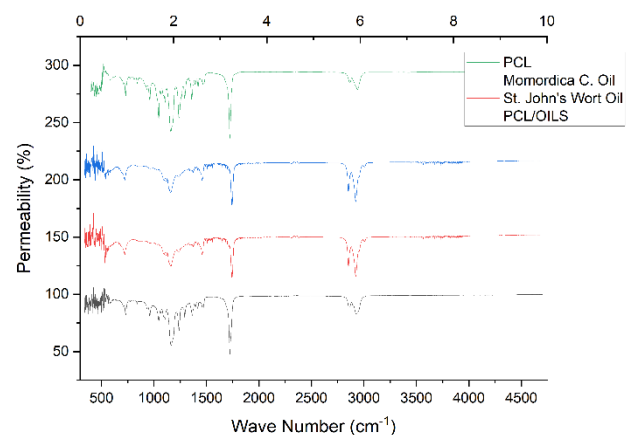
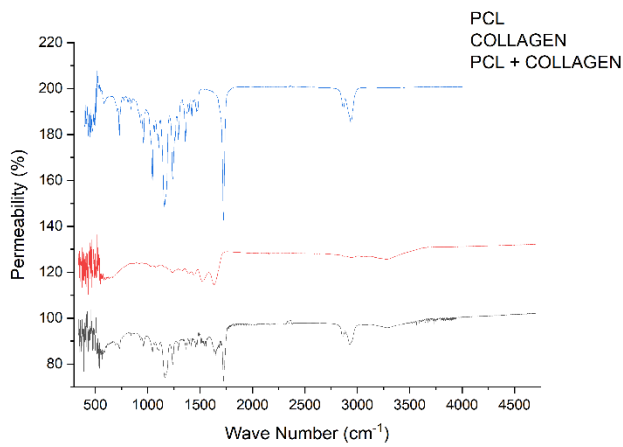


Figure 1. FTIR spectrums of nanofiber, Momordica C. Oil, St John's Wort Oil, PCL.



**Figure 2.** FTIR spectrums of nanofiber, Collagen, PCL.

**B. Field Emission Scanning Electron Microscope (FE-SEM)**

FE-SEM images of nanofibers containing PCL, collagen and oils are demonstrated in Figure 3.

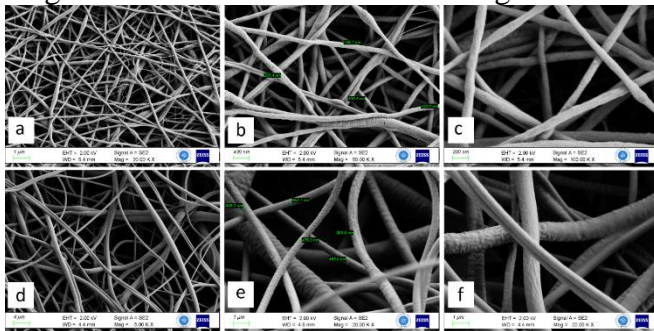


**Figure 3.** SEM images (a,b and c first layer, d,e,f second layer)

**C. Thermogravimetric Analysis Results**

In Figure 4, thermal degradation curves of PCL/Oils, PCL/COL and final nanofiber product prototype are given. Based on the graphs formed as a result of the analysis, the temperature range, thermal degradation range and weight loss of the nanofibers were calculated.

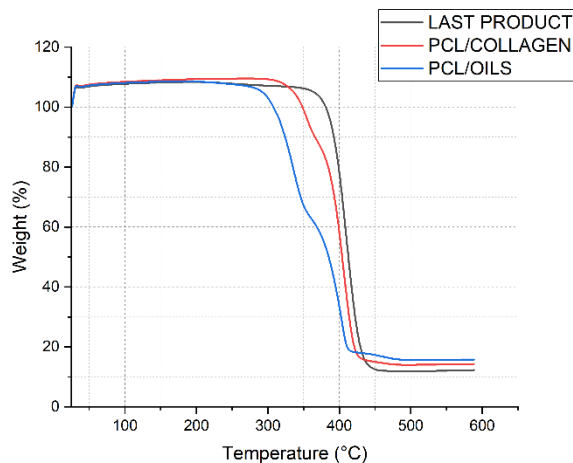


**Figure 4.** Thermogravimetric degradation curves of PCL/COL, PCL/Oils, final product prototype nanofibers

**D. Mechanical tensile test**

Mechanical tensile tests of the fabricated PCL/Oils, PCL/COL and final product prototype were carried out at constant tensile speed of 5 mm/minute after samples were cut 1/5 of template, and the stress-strain curves were plotted as seen in Figure 5. In Table 1, the maximum stress, maximum strain and Young's modulus values of each nanofiber are given.

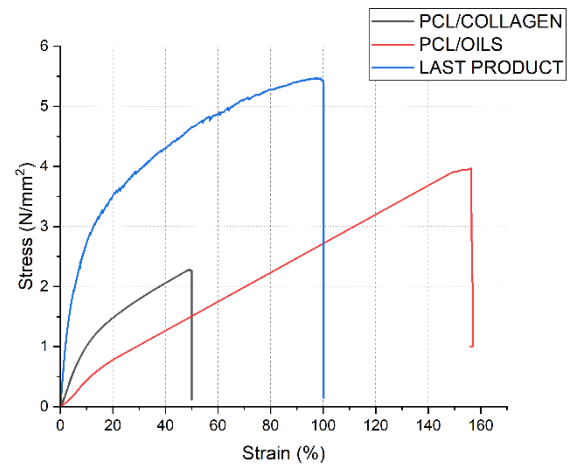


**Figure 5.** Strain of PCL/OILS, PCL/COL, product prototype nanofibers

**Table 1.** Maximum stress, maximum strain and Young's modulus values of nanofibers

Nanofiber	Max. Stress (N/mm <sup>2</sup> )	Maks. Strain (%)	Young's Modulus (Mpa)
PCL/Oils	3.97	156.95	4.88
PCL/COL	2.28	49.19	5.4
Final product prototype	5.47	100.25	15.41

**E. In Vitro Biocompatibility Test**

When normal fibroblast cells were produced together with nanofibers, they demonstrated 60.40% proliferation at 24th hour, 80.18% at 72nd hour and 66.71% at 144th hour when compared to control.

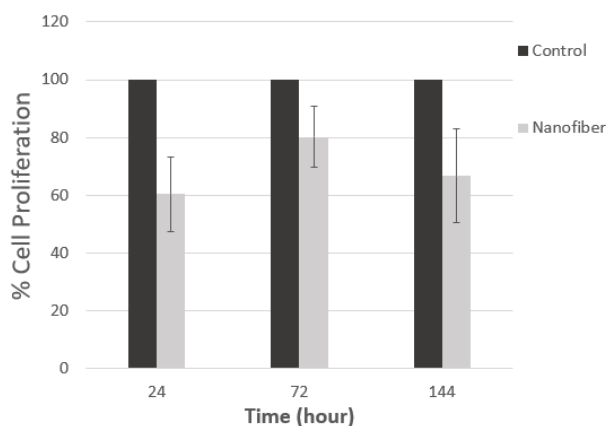


**Figure 6.** % proliferation of L929 cells after incubation with prototype for different periods.

#### IV. DISCUSSION

The FTIR spectrum plot of PCL nanofiber is shown in Figure 4.4 and it has been determined as a result of the researches that characteristic peaks are from  $\text{CH}_2$  vibration at  $732\text{ cm}^{-1}$ , C–O–C symmetric bond at  $961\text{ cm}^{-1}$ , C–C bond at  $1364\text{ cm}^{-1}$ ,  $1140\text{ cm}^{-1}$ . C–O bond at  $1161\text{ cm}^{-1}$ , points  $1239$  and  $1293\text{ cm}^{-1}$  representing stretching of PCL in the crystal phase from C–C and C–O bond, respectively, and symmetrical deformation of the C–H bond at  $1364\text{ cm}^{-1}$ , C=O stretching vibration at  $1720\text{ cm}^{-1}$ , C–H<sub>2</sub> symmetrical stretching vibration at  $2865\text{ cm}^{-1}$ , and C–H<sub>2</sub> asymmetrical stretching vibration at  $2942\text{ cm}^{-1}$  [6]. When the FTIR spectra of nanofibers and oils are considered together in Figure 1, it shows that nanofiber exhibits a balanced structure with nanofibers without causing any deterioration of oils in functional groups. In Figure 2, it is seen that the permeability percentage of PCL/COL nanofibers decreased compared to PCL nanofiber and there was a clear difference in wavenumbers, PCL polymer was suppressed by collagen.

Random and interconnected fibrous meshes with fiber diameters in the nanometer range were obtained by electrospinning. SEM images showed that the obtained nanofibers were composed of beadless, smooth fibers. The PCL/COL nanofiber size used in the first layer (Figure 3. a, b, c) was obtained as approximately 135 nm. The nanofiber size (Figure 3. d, e, f) of PCL, St. John's Wort oil and *Momordica Charantia* maceration oil used in the second layer was obtained as approximately 513 nm. These results showed that the fats were well incorporated into the fibers and the mean diameter increased as the amount of fat increased.

Weight losses occurred at the temperature ranges of  $275\text{-}410\text{ }^\circ\text{C}$ ,  $300\text{-}430\text{ }^\circ\text{C}$  and  $350\text{-}440\text{ }^\circ\text{C}$  for PCL/Oils, PCL/COL and the final product nanofiber prototype, respectively. Weight losses due to temperature increase were found to be approximately 88.4%, 84.32% and 88.1% for PCL/Oils, PCL/COL and final product nanofiber prototype, respectively. The sample with the lowest thermal stability is PCL/Oils, they started to decompose at lower temperatures than the other samples showed decomposition. The sample with the highest thermal stability is the final product. The final product is nanofiber, which starts to degrade at higher temperature compared to other samples.

Maximum tensile values were found as 3.97 MPa, 2.28 MPa and 5.47 MPa for PCL/Oils, PCL/COL and final product nanofiber prototype, as given in Table 4.3. Maximum elongation values were found to be 156.95%, 49.19% and 100.25% for PCL/Oils, PCL/COL and final product prototype nanofibers, respectively. When the tension curves of the nanofibers are compared, it is seen that the nanofiber of the final product has the highest tension with 5.47 Mpa, and then the highest tension value is followed by the PCL/Oils nanofiber with 3.97 MPa.

PCL is a hydrophobic material and there is little difference in mechanical properties between the dry and wet state. Collagen has a natural tendency to absorb fluid, which increases its elasticity [7]. The reason why the strength value of PCL/COL nanofibers is lower than PCL/Oils nanofiber is due to the fact that collagen cannot form a good bond in thermoplastic PCL. Thus, it deteriorated the structural bond integrity of the nanofiber and caused it to show lower strength [8].

When fibroblast cells were produced together with nanofibers, they showed 60.40%, 80.18% and 66.71% proliferation after 24-, 72- and 144-hours incubation with prototype, respectively. The cell proliferation higher than 50% means that the treatment material did not exert any significant toxicity to the proliferating cells. It may be deduced that the dressing does not have a toxic effect and is biocompatible with normal fibroblast cells.

#### V. CONCLUSION

The results reveal that nanofibers prepared with PCL/St. John's Wort oil/*Momordica charantia* maceration oil and PCL/COL have promising

potential for wound healing applications. In future studies, the wound healing potential of the prototype will be tested on three-dimensional wound model.

#### ACKNOWLEDGMENT

This project was supported by the project No. ZV-AGM-2018-1/AG-132 (Development of Pharmaceutical Wound Bed Dressing Prototype in accordance with European and American Pharmacopoeias that Accelerate Wound Healing Process with Phenolic Components) and also supported by TUBITAK 2244 University Industry Collaboration Project (119C100).

We gratefully acknowledge Zade & Zade Vital İbn-i Sina R&D Center for their support.

#### REFERENCES

- [1] Tottoli, E. M., Dorati, R., Genta, I., Chiesa, E., Pisani, S., & Conti, B. (2020). Skin Wound Healing Process and New Emerging Technologies for Skin Wound Care and Regeneration. *Pharmaceutics*, 12(8). doi:10.3390/pharmaceutics12080735
- [2] Fahimirad, S., & Ajalloueiian, F. (2019). Naturally-derived electrospun wound dressings for target delivery of bio-active agents. *Int J Pharm*, 566, 307-328. doi:10.1016/j.ijpharm.2019.05.053
- [3] Kanikireddy, V., Varaprasad, K., Jayaramudu, T., Karthikeyan, C., & Sadiku, R. (2020). Carboxymethyl cellulose-based materials for infection control and wound healing: A review. *Int J Biol Macromol*, 164, 963-975. doi:10.1016/j.ijbiomac.2020.07.160
- [4] Zhao, Y. T., Zhang, J., Gao, Y., Liu, X. F., Liu, J. J., Wang, X. X., . . . Long, Y. Z. (2020). Self-powered portable melt electrospinning for in situ wound dressing. *J Nanobiotechnology*, 18(1), 111. doi:10.1186/s12951-020-00671-w
- [5] Altan, A., Damlar, İ., Aras, M. H., & Alpaslan, C. (2015). Sarı Kantaronun (*Hypericum Perforatum*) Yara İyileşmesi Üzerine Etkisi. *Arşiv Kaynak Tarama Dergisi*, 24 (4), 578.
- [6] Shalumon, K. T., Sreerekha, P. R., Sathish, D., Tamura, H., Nair, S. V., Chennazhi, K. P., & Jayakumar, R. (2011). Hierarchically designed electrospun tubular scaffolds for cardiovascular applications. *J Biomed Nanotechnol*, 7(5), 609-620. doi:10.1166/jbn.2011.1337
- [7] Lee SJ, Liu J, Oh SH, Soker S, Atala A, Yoo JJ. (2008). Development of a composite vascular scaffolding system that withstands physiological vascular conditions. *Biomaterials*. 29(19):2891–2898
- [8] Xia, D., Zhang, S., Hjortdal, J. Ø., Li, Q., Thomsen, K., Chevallier, J., ... & Dong, M. (2014). Hydrated human corneal stroma revealed by quantitative dynamic atomic force microscopy at nanoscale. *ACS nano*, 8(7), 6873-6882.